

Spatially-selective amplified spontaneous emission source derived from an ultra-high gain solid-state amplifier

G. Smith and M. J. Damzen

The Blackett Laboratory, Imperial College London, London, SW7 2BW, UK
gerald.smith@imperial.ac.uk

Abstract: An investigation is made into the performance of a high power solid-state amplified spontaneous emission (ASE) source with near-diffraction-limited beam quality. The radiation from this ASE source has high spatial quality and power, but unlike a laser it has a high misalignment tolerance and does not require a precisely aligned cavity. The source is based on a diode-pumped Nd:YVO₄ laser crystal in a bounce amplifier geometry with a uniquely ultra-high gain ($\sim 10^4$ - 10^5). Double-pass ASE radiation with high power levels (>6 W) is achieved in a near-diffraction-limited spatial quality. We further demonstrate that the double-pass ASE source also displays high spatial selectivity and capability to compensate for a phase diffuser, inserted in the double-pass arm, with only a small degradation in beam quality and power.

© 2006 Optical Society of America

OCIS codes: (140.3580) Lasers, solid-state; (140.6630) Superradiance, superfluorescence; (140.3480) Lasers, diode-pumped; (140.3530) Lasers, neodymium.

References and links

1. A. Siegman, *Lasers* (University Science Books, California, 1986), Chap. 13.
2. O. Svelto, *Principles of Lasers* (Plenum Press, New York and London, 1998), Chap. 2.
3. A. Yariv and R. C. Leite, "Super Radiant Narrowing in Fluorescence Radiation of Inverted Populations," *J. Appl. Phys.* **34**, 3410-3411 (1963).
4. P. Ewart, "A modeless, variable bandwidth, tunable laser," *Opt. Commun.* **55**, 124-126 (1985).
5. S. Tsai, T. Tsai, P. Law, and Y. Chen, "High Pumping-Efficiency L-Band Erbium-Doped Fiber ASE Source Using Double-Pass Bidirectional-Pumping Configuration," *IEEE Photonics Technol. Lett.* **15**, 197-199 (2003).
6. J.E. Bernard and A.J. Alcock, "High-efficiency diode-pumped Nd:YVO₄ slab laser," *Opt. Lett.* **18**, 968-970 (1993).
7. A. Minassian, B. Thompson, and M.J. Damzen, "Ultrahigh-efficiency TEM₀₀ diode-side-pumped Nd:YVO₄ laser," *Appl. Phys. B* **76**, 341-343 (2003).
8. A. Minassian, B. Thompson, and M.J. Damzen, "High-power TEM₀₀ grazing-incidence Nd:YVO₄ oscillators in single and multiple bounce configurations," *Opt. Commun.* **245**, 295-300 (2005).
9. O. Svelto, S. Taccheo, and C. Svelto, "Analysis of amplified spontaneous emission: some corrections to the Linford formula," *Opt. Commun.* **149**, 277-282 (1998).
10. W. Koechner, *Solid-State Laser Engineering* (Springer-Verlag, Berlin, 1999), Chap. 3.

1. Introduction

In an optical amplifier, spontaneous emission (SE) can receive amplification along the length of the gain medium and become quite powerful; it is known as amplified spontaneous emission (ASE) or super-fluorescence [1]. In most laser systems ASE is viewed as an unwanted parasitic effect and measures taken to minimise it. However, ASE can also be exploited in a high gain amplifier with the correct geometry to achieve intense radiation with high directionality, without the need for cavity mirrors [2,3]. A few practical implementations

of high spatial quality ASE sources have been in high gain pulsed amplifier systems including dye lasers [4] and continuous wave single mode fibre sources [5]. To date, however, no demonstrations have been made on solid-state lasers due to low gain and/or poor geometry (e.g. large aperture rods).

In this paper we present, for the first time to our knowledge, a detailed investigation of a high power solid-state ASE source with high spatial quality. By using an ultra-high gain ($\sim 10^4$ - 10^5) Nd:YVO₄ bounce amplifier [6-8] in a double-pass ASE geometry, we achieve 6.3W of near-diffraction-limited beam quality. We investigate the geometry to show that the high beam quality can be explained by self-spatial filtering. The system is highly tolerant to misalignment and, more surprisingly, we show that when a phase distorter is placed in the double-pass arm, little reduction in beam quality and power level is produced in the ASE output. The usefulness of the source is demonstrated as its output has a high tolerance to system misalignment and to external perturbations. The system demonstrates a high spatial selectivity, ability for compensation of phase distortions and the potential for creating high quality radiation sources that lift the cavity stability and precision alignment constraints required of conventional laser resonators.

2. Single-pass ASE in Nd:YVO₄ bounce amplifier geometry

2.1 Nd:YVO₄ bounce amplifier geometry

The solid-state amplifier under investigation is a diode-pumped Nd:YVO₄ crystal in a bounce amplifier configuration, as shown in Fig. 1. The Nd:YVO₄ crystal is an *a*-cut slab (crystal is cut perpendicular to the *c*-axis which is the optic axis) with dimensions 20 x 5 x 2mm (length x width x height) and 1.1 at. % neodymium doping. It is diode-pumped at 808nm and its main lasing transition is at 1064nm. The two 5 x 2mm end faces are anti-reflection (AR) coated for 1064nm. The slab is diode-pumped on the 20 x 2mm front face, which is AR coated for 808nm. The pump diode has fast axis collimation and is focused onto the front face with a $f=12.7$ mm vertical cylindrical lens (VCL_D) producing a line focus with dimensions ~ 15 x 0.1mm. The light output from the laser diode is polarised parallel to the *c*-axis of the crystal hence accessing the high absorption coefficient of $\sim 30\text{cm}^{-1}$ for 1.1 at. % Nd:YVO₄ and resulting in strong absorption of pump power, with absorption depth $\sim 330\mu\text{m}$.

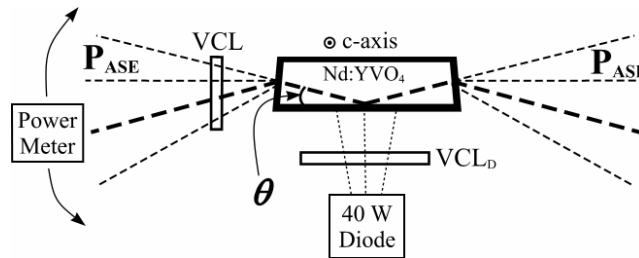


Fig. 1. Schematic diagram for measurement of angular-dependence of single-pass ASE power, P_{ASE} . VCL is a vertical cylindrical lens of focal length $f=60$ mm to aid collection of radiation to diagnostics.

In the bounce geometry employed in the crystal, radiation can be amplified by taking a path that experiences total internal reflection at the pump face [6-8]. The bounce angles (θ) with respect to the crystal's pump face give considerable spatial averaging of the gain and thermal non-uniformities seen by the amplified beam in the bounce plane. However, the key significance to this geometry is its ability to produce extremely high gain ($\sim 10^4$ - 10^5).

The ASE intensity, I , for a cylindrical rod amplifier with uniform gain, is given by [9]

$$I = \phi I_s \left(\frac{\Omega}{4\pi} \right) \frac{(G-1)^{3/2}}{(G \ln G)^{1/2}} \quad (1)$$

in which $G=\exp(\sigma_p Nl)$ is the peak unsaturated gain of the amplifier (where σ_p is the peak emission cross-section, N is the inversion density and l is the length of the active medium), $I_s=hv_0/\sigma_p\tau$ is a characteristic saturation intensity of the transition (where v_0 is the peak transition frequency and τ is the transition lifetime), Ω is the solid angle subtended by one end of the gain region as seen from the central point of the opposite end and ϕ is the fluorescence quantum yield ($\phi=\tau A$, where A is the rate of spontaneous emission).

For high gains where $G\gg 1$, the ASE intensity may be well approximated by

$$I = \phi I_s \left(\frac{\Omega}{4\pi} \right) \frac{G}{(\ln G)^{1/2}} \quad (2)$$

For the slab bounce geometry, gain is not uniformly distributed so the calculation of solid angle and hence ASE intensity must be modified somewhat, as discussed in the next section.

2.2 Single-pass ASE experimental results

As indicated in Fig. 1, when diode-pumped, the crystal is observed to emit ASE in a large range of angles corresponding to different internal bounce angles θ in the crystal. A power meter with circular aperture (diameter 9mm) placed at a distance of 600mm from the laser crystal was used to measure the horizontal angular dependence θ of the ASE power. A vertical cylindrical lens (VCL) was used to collect all the vertical component of the ASE onto the aperture of the power meter.

Figure 2 shows experimental results of measured ASE power against internal bounce angle θ for different diode-pumping powers from 20-35W. Strong single-pass ASE (SP-ASE) powers are observed. Maximum ASE power of 158mW is obtained at 1.5° for 35W pumping. Power decreases markedly between θ in the range $\sim 1.5^\circ$ - 4° , more weakly from 4° - 9° , and appears approximately constant between 10° - 14° . For $\theta < 1.5^\circ$, a fall-off in power is observed.

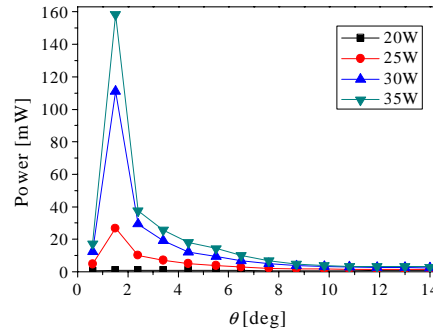


Fig. 2. Experimental results of SP-ASE power against bounce angle θ .

To compare ASE powers with the theoretical formula Eq. (2) for high gain ASE, the specific geometry of the bounce amplifier must be considered carefully. The gain region has a length $L\sim 15$ mm, vertical dimension $d_v\sim 0.1$ mm and horizontal dimension $d_H\sim 0.33$ mm (absorption depth). The highest gain would be expected in the solid angle $\Omega=\theta_H$. $\theta_v=(2d_H/L)$. $(d_v/L)=2.9\times 10^{-4}$ steradians, where the extra factor of two for the horizontal dimension accounts for the increased angular range (θ_H) due to total internal reflection in this plane. The horizontal angular extent $\theta_H\sim 2.5^\circ$ corresponds well to the observed experimental angular region of highest ASE output power. As may be seen from Fig. 1, for smaller bounce angles, radiation is incident on the crystal end face closer-and-closer to the end corner. The fall-off in ASE power for $\theta < 1.5^\circ$ is therefore believed to be due to losses due to diffractive clipping at the corners of the crystal ends. For Nd:YVO₄, taking $\sigma_p\sim 15\times 10^{-19}$ cm² and $\tau\sim 90\mu$ s, gives $I_s\sim 1.4$ kW/cm². Single-pass gain measurements give a value of gain $G_{SP}\sim 2\times 10^4$ for $\theta=4^\circ$

at 25W diode pump power, making the high gain approximation of Eq. (2) valid. Assuming the beam size at exit crystal face is $\sim 0.33\text{mm}$ in the horizontal and $\sim 100\mu\text{m}$ in the vertical, and taking a fluorescence quantum yield $\phi \sim 0.6$, gives a value for the total ASE power of $\sim 40\text{mW}$ for 25W diode pump power. This is consistent with the ASE power at this pump power.

3. Double-pass ASE bounce amplifier device

3.1 Double-pass ASE configuration

The experimental configuration used for double-pass ASE (DP-ASE) is shown in Fig. 3. By insertion of a mirror (M1) of reflectivity $R=100\%$ at a distance d from the amplifier to reflect the SP-ASE, a small solid angle is defined through which radiation may pass through the amplifier for a second time experiencing double-pass gain.

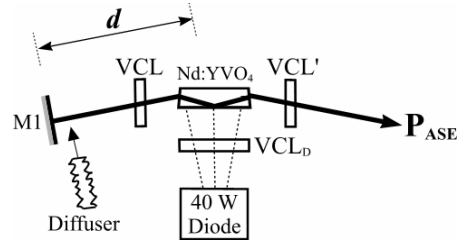


Fig. 3. Experimental set-up for DP-ASE bounce amplifier configuration. VCL and VCL' are vertical cylindrical lenses of focal lengths $f=60\text{mm}$.

All experimental features of the bounce amplifier are identical to the case described earlier in the SP-ASE experiment. One addition is a second vertical cylindrical lens VCL' placed as shown on the right hand side of the Nd:YVO₄ crystal to aid light collection to the diagnostics. Both VCL and VCL' are AR coated at 1064nm and were angled away from normal incidence to prevent direct Fresnel reflections being re-incident through the crystal and also to minimise scatter feedback.

Figure 4 shows experimental results of DP-ASE power against θ (selected by orientation of M1) for a pumping power range of 20-35W, for mirror distance $d=150\text{mm}$.

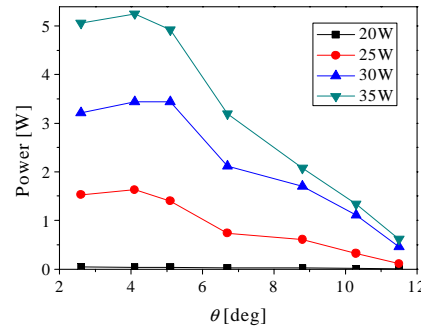


Fig. 4. Experimental results of DP-ASE power against θ .

Powers up to 5.2W at 4.1° are achieved at 35W pumping. This can be compared to 158mW at 1.5° for the SP configuration (Fig. 2). The important feature is that in the DP-ASE configuration watts of power are produced compared to milliwatts for the SP-ASE case.

In a similar way to the SP-ASE case, the ASE intensity can be calculated but using a solid angle (Ω) subtended by the apparent aperture of the bounce amplifier over the double-pass length $2d$. For the case of M1 selecting a bounce angle $\theta=4^\circ$, the apparent size of the gain region along the pump face (15mm) appears as a limiting aperture $d_H \sim 1\text{mm}$ in the horizontal,

and gain region has a vertical aperture size $d_v \sim 0.1\text{mm}$. For $d=150\text{mm}$, the double-pass horizontal angle subtended $\theta_H \sim d_H/2d = 1\text{mm}/300\text{mm} = 0.0033\text{rad}$ and in the vertical, $\theta_V \sim 100\mu\text{m}/15\text{mm} = 0.0067\text{rad}$ (identical to SP-ASE case due to the collimating lens VCL). For SP gain $G_{SP} \sim 2 \times 10^4$, then DP gain is $G_{DP} \sim G_{SP}^2 \sim 4 \times 10^8$. This leads, via Eq. (2), to a predicted DP-ASE power of $\sim 45\text{W}$. This value is clearly unphysical, but the theory is based on the non-gain saturation regime. This calculation shows that the amplifier is expected to be highly saturated and is consistent with the observed multiwatt DP-ASE output power.

3.2 Spatial and spectral characteristics of DP-ASE

An investigation was made of the spatial quality of the DP-ASE output, at a bounce angle of 4° . For $d=150\text{mm}$, the spatial output is of a high quality with beam propagation parameter M^2 measurements giving values of $M^2 < 2$ (horizontal) and < 1.2 (vertical), corresponding to close to diffraction-limited spatial form. In general, as d is reduced, the power increases as diffractive losses are less. Spatial quality is approximately constant as a function of d , until a distance of approximately 100mm where the beam starts to become degraded in the horizontal. This high spatial quality for longer path lengths (d) is attributed to spatial filtering of the ASE. Near-diffraction-limited beam quality is expected when Fresnel number $N_F = a^2/\lambda(2d)$ is less than unity, where a is the limiting aperture size of the amplifier.

Spectrally, the output was investigated by use of a Fabry-Perot etalon. At higher pump powers the spectrum jitters between broadband emission and defined modal structure. Analysis of the mode spacings indicates the modes correspond to distances between M1 and VCL', and the crystal end faces and the VCLs. This was also confirmed by monitoring the timescales of the temporal mode beating in output power on a fast detector and oscilloscope.

The AR-coated lens VCL' was angled at $\sim 10^\circ$ to the beam path so specular reflection could not be the cause of the modal structure. To investigate further, we performed a separate experiment to measure the strength of the diffuse scatter of the lens VCL' that could effectively re-inject the DP system. A diffuse backscatter reflectivity of 2×10^{-3} per steradian was measured for VCL', at orientation 5° - 10° . For the DP-ASE geometry employed (VCL' located at a distance $l'=60\text{mm}$ from the laser crystal and $d=150\text{mm}$), the total solid angle for double-pass diffuse backscatter is $\Omega' = 4.6 \times 10^{-6}$ steradians. This leads to an effective diffuse DP reflectivity $R_{DP} \sim (2 \times 10^{-3}/\text{sr}) \times (4.6 \times 10^{-6}\text{sr}) \sim 10^{-8}$. For a standard laser oscillator with mirror reflectivities R_1 and R_2 and double-pass gain G_{DP} , the lasing threshold condition is $R_1 R_2 G_{DP} = 1$ [10]. For the DP set-up, with reflectivity $R_1 = 1$ and $R_2 = R_{DP} = 10^{-8}$ and gain $G_{DP} \sim 4 \times 10^8$, it is found that even with such a weak diffuse scatter from VCL', the system is above laser threshold. This would account for the presence of the modal features.

3.3 Spatial selectivity of DP configuration

The DP-ASE system is shown to be able to produce high spatial quality. This is expected due to spatial filtering as the DP-ASE system selects a low divergence component of the ASE that will receive enhanced DP gain. To investigate the spatial selectivity process further we placed a phase diffuser plate near mirror M1. The diffuser had a 0.5° diffusion angle. Mirror M1 was placed at $d=225\text{mm}$. Output power (Fig. 5(a)) and spatial quality (Fig. 5(b)) of the DP-ASE were measured with and without the presence of the diffuser, as shown in Fig. 5. Without the diffuser, output power 6.3W is produced with $M^2 < 1.8$ in the horizontal and < 1.2 in the vertical. With diffuser included, output power only reduces by $\sim 7\%$ to 5.8W . Horizontally, M^2 increases from < 1.8 to < 2.0 , which is only a small degradation. Vertically, M^2 is unaffected.

To understand how the system is able to maintain its performance we propose the following explanation. ASE at the mirror is composed of a complex (partially coherent) and divergent spatial form. If no diffuser is present, the lowest divergence component of the ASE in the reverse direction to the mirror is selected in double-pass of the gain. If a diffuser is added at the mirror, the lowest divergence component of the ASE is not the favoured spatial configuration due the subsequent distortion. A better selected component will be an aberration-reversed version of the double-pass distortion; effectively the system picks out the

phase conjugate solution from the many possible components of the single-pass ASE, such that low divergence radiation is selected *after* double-pass of the diffuser.

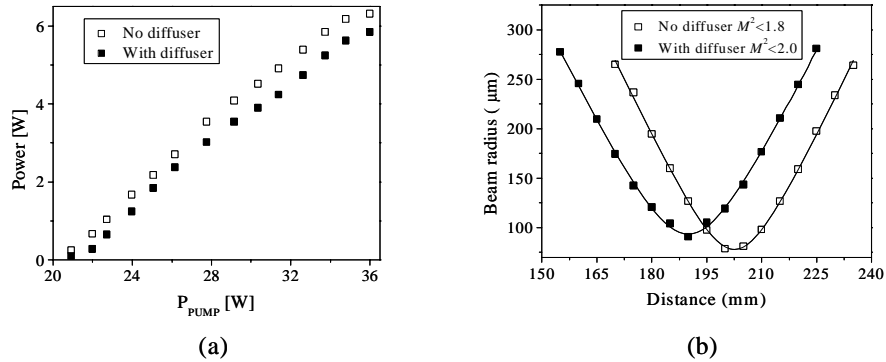


Fig. 5. Experimental results of: (a) DP-ASE power against pump power with diffuser, (b) horizontal beam radius through focus for M^2 measurement.

Figure 6 shows the spatial form of the DP-ASE output. Three traces are shown: (a) without the diffuser, (b) with diffuser at M1 and (c) with diffuser in the output beam prior to the camera. It may be seen that with diffuser at M1, the spatial form is not significantly degraded. A small change in beam size appearance (comparing Fig. 6(a) to 6(b)) appears to be caused by the diffuser changing the beam radius of curvature slightly. The severity of the diffuser on the output beam is shown in Fig. 6(c). These results indicate the ability of the DP system to compensate for the diffuser.

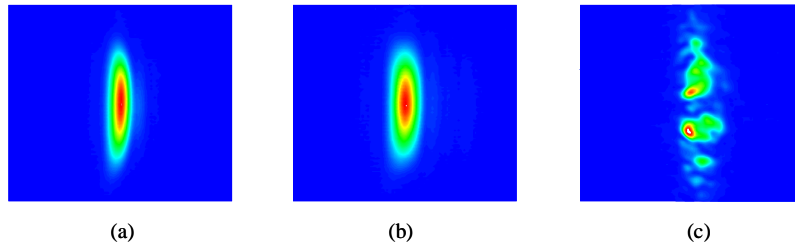


Fig. 6. Spatial forms: (a) without diffuser, (b) with diffuser at M1, (c) with diffuser in output.

4. Conclusion

An investigation is made of a high power solid-state laser amplified spontaneous emission (ASE) source. The novel source is based on an ultra-high gain ($\sim 10^4$ - 10^5) diode-pumped Nd:YVO₄ laser crystal, in a bounce amplifier geometry. Single-pass and double-pass configurations are investigated. Double-pass ASE radiation with high power levels ($>6\text{W}$) is achieved in a near-diffraction-limited spatial quality, with horizontal $M^2 < 1.8$ and vertical $M^2 < 1.2$. We demonstrate that the double-pass ASE source also displays high spatial selectivity and capability to compensate for a phase diffuser, inserted in the double-pass arm, with only a small degradation in beam quality and power. This work indicates the potential for creating high quality radiation sources that remove the requirements for cavity stability and precision alignment constraints of conventional laser resonators.

Acknowledgements

The authors acknowledge support from The Engineering and Physical Sciences Research Council (UK) under grant number GR/T08555/01. G. Smith's email address is gerald.smith@imperial.ac.uk.